

# The Ionospheric Impact of the October 2003 Storm Event on WAAS

Attila Komjathy, Lawrence Sparks, Anthony J. Mannucci  
*Jet Propulsion Laboratory/ California Institute of Technology*  
*M/S 238-600, 4800 Oak Grove Drive, Pasadena, CA 91109*

Anthea Coster  
*MIT Haystack Laboratory, Atmospheric Sciences*  
*Westford, MA 01886*

## BIOGRAPHIES

Attila Komjathy is currently a staff member of the Ionospheric and Atmospheric Remote Sensing (IARS) Group of the Tracking Systems and Applications Section at Jet Propulsion Laboratory (JPL), specializing in remote sensing techniques using the Global Positioning System. Prior to his joining JPL in July 2001, he worked on the utilization of GPS reflected signals as a Research Associate at the University of Colorado's Center for Astrodynamics Research. He received his Ph.D. from the Department of Geodesy and Geomatics Engineering of the University of New Brunswick, Canada in 1997.

Lawrence Sparks is a senior member of the IARS Group at JPL. He received his Ph.D. in Applied Physics from Cornell University. His published research has spanned fields including fusion plasma physics, solar magneto-hydrodynamics, atmospheric radiative transfer, and ionospheric modeling. He is currently working on applications of GPS to ionospheric science.

Anthony J. Mannucci is supervisor of the IARS Group at JPL. He has developed ionospheric calibration systems for deep space tracking and Earth science applications. He works with the Federal Aviation Administration on the Wide Area Augmentation System differential GPS implementation and is a member of the international ionospheric working group for Satellite-Based Augmentation Systems (SBAS). He obtained a Ph.D. in Physics from U.C. Berkeley in 1989.

## ABSTRACT

The United States Federal Aviation Administration's (FAA) Wide Area Augmentation System (WAAS) for civil aircraft navigation is focused primarily on the Conterminous United States (CONUS). Other Satellite-

Based Augmentation Systems (SBAS) include the European Geostationary Navigation Overlay Service (EGNOS) and the Japanese Global Navigation Satellite System (MSAS). Navigation using WAAS requires accurate calibration of ionospheric delays. To provide delay corrections for single frequency GPS users, the wide area differential GPS systems depend upon accurate determination of ionospheric total electron content (TEC) along radio links. Dual-frequency transmissions from GPS satellites have been used for many years to measure and map ionospheric TEC on regional and global scales.

The 2003 October solar-terrestrial events are significant not only for their dramatic scale, but also for their unique phasing of solar irradiance and geomagnetic events. During October 28, the solar X-ray and EUV irradiances were exceptionally high while the geomagnetic activity was relatively normal. Conversely, October 29-31 was geomagnetically active while solar irradiances were relatively low. These events had the most severe impact of recent history on the CONUS region and therefore had a significant effect on the WAAS performance. To help better understand the event and its impact on WAAS, we examine in detail the WAAS reference site (WRS) data consisting of triple redundant dual-frequency GPS receivers at 25 different locations within the US. To provide ground-truth, we take advantage of the three co-located GPS receivers at each WAAS reference site.

To generate ground-truth and calibrate GPS receiver and transmitter inter-frequency biases, we process the GPS data using the Global Ionospheric Mapping (GIM) software developed at the Jet Propulsion Laboratory. This allows us to compute calibrated high resolution observations of TEC.

We found ionospheric range delays up to 35 meters for the day-time CONUS during quiet and up to 100 meters during storm time conditions. For quiet day, we obtained

WAAS planar fit slant residuals less than 2 meters (0.4 meter RMS) and less than 20 meters (3.5 meter RMS) for the storm day. We also investigated ionospheric gradients, averaged over a distances of a few hundred km. The gradients were no larger than 0.5 meter over 100 km for a quiet day. For storm day, we found gradients at the 4 meter level over 100 km. Similar level gradients could only be typically observed in low latitude region.

## INTRODUCTION

The Wide-Area Augmentation System (WAAS) developed for the Conterminous United States (CONUS) is only one of the several Space-Based Augmentation Systems (SBAS) under consideration worldwide. Other SBAS developments are under way in Europe, Japan, India and Brazil.

Relatively benign ionospheric conditions in the mid-latitude CONUS region are compatible with accurate ionospheric range corrections for WAAS. Providing ionospheric corrections for disturbed days is significantly more challenging. Major storm events such as the one on October 29-31, 2003 show absolute ionospheric delays and gradients similar to those that can only be observed in the equatorial region.

The ionosphere has been extensively studied to support WAAS at the CONUS sector. The published literature discussing ionospheric corrections for WAAS in the CONUS is extensive; see e.g. Enge et al., [1996], WAAS MOPS [1999], Walter et al., [2000]. Various alternative ionospheric correction algorithms have been presented by e.g., Sparks et al., [2000, 2004a, 2004b], Blanch et al., [2002] and Komjathy et al., [2003a].

In Komjathy et al., [2003b], we assessed the WAAS planar fit algorithm in the equatorial region where the spatial gradients and the absolute slant TEC are known to be the highest in the world. We found that in the equatorial region the dominant error source for the WAAS planar fit algorithm is the inherent spatial variability of the equatorial ionosphere, with ionospheric slant range delay residuals as high as 15 meters and root-mean square (RMS) residuals for the quiet day of 1.9 meters. This compares to a quiet-day maximum residual of 2 meters in CONUS, and 0.5 meter RMS. We revealed that ionospheric gradients in the equatorial region are, on average, at the level of 2 meters over 100 km. Contrary to results obtained for CONUS, we discovered that a major ionospheric storm (March 31, 2001) had small impact on the planar fit residuals in the low latitude sector.

In a follow-up investigation in Komjathy et al., [2003c], we investigated major storm events of the last few years and evaluated their impact on WAAS ionospheric model performance in Brazil, Europe and CONUS. These storms included the “worst-case” CONUS storms such as those on July 15, 2000, and March 31, 2001; we investigated their impact on SBAS in Europe and Brazil. Results indicated that lesser known storms such as the one on April 5, 2000 had a more significant impact in Europe than a near worst-case storm in CONUS. Furthermore, in terms of planar fit residuals, we provided additional evidence that there is little difference between quiet and storm time behavior over Brazil. We found that the Brazilian planar fit residuals are 2 to 4 times higher (RMS) than those for Europe and CONUS.

Following these previous investigations, quite unexpectedly, one of the most exciting solar-terrestrial space weather event in recent history took place on October 29-31, 2003. The storm event had a major impact on the CONUS region that we had not seen in the CONUS region before and it can only be matched by events in the equatorial region. In this research, we will compare slant ionospheric delays and planar fit residuals with those of other CONUS storm event. We will also relate these to storm events observed in the equatorial region.

To establish a background for this work, we first review the estimation method that uses a network of 75 WAAS Reference Element (WRE) receivers located at 25 WRS locations (three co-located WRE receivers at each WRS). We have generated a ground-truth data set using all 75 WRE receivers. We briefly describe the algorithm we use to estimate satellite and receiver interfrequency biases then a voting scheme is used to select one of the three threads to serve as a truth measurement.

## GENERATING HIGH PRECISION TEC DATA

The algorithm comprises two main parts. First, a highly precise interfrequency bias estimation part that applies existing technology using GIPSY and GIM software packages. The 1-second RINEX data is cleaned and decimated to 300 seconds and passed through a sequential least squares estimator to obtain high precision satellite and receiver differential biases. Secondly, we post-process the raw GPS data using nearly co-located GPS receivers to obtain highly precise leveled phase ionospheric measurements not available in real-time.

During subsequent post-processing steps, we correct the measurements for the satellite and receiver interfrequency biases, estimated in the previous step to obtain the unbiased line-of-sight total electron content measurements. The cleaned data sets are then passed through a voting algorithm to select one of the three thread measurements to serve as a ground truth. The output of this process is the final “truth” data, intended to serve as ground-truth for WAAS algorithm development and validation purposes.

*Interfrequency bias estimation.* Ionospheric measurements from a GPS receiver can be modeled with the well-known single-shell ionospheric model. [see e.g. Mannucci et al., 1999 and Komjathy et al., 2002]. The dependence of vertical TEC on latitude and longitude is parameterized as a linear combination of the two-dimensional basis functions  $B_i$ , which are functions of solar-geomagnetic longitude and latitude [Mannucci et al., 1998] (We note that the summation in Equation 1 is over all basis functions  $B_i$ ). Using the carrier phase-leveled ionospheric GPS observables, a Kalman filter simultaneously solves for the instrumental biases and the coefficients  $C_i$ , which are allowed to vary in time as a random walk stochastic process [Iijima et al., 1999]. The basis functions currently used are based on a bicubic spline technique developed at JPL [Lawson, 1984].

*Preprocessing RINEX Data.* To generate high precision ionospheric TEC data, we use 36-hour RINEX files with 1 second sampling rate using all 75 WRE receivers. In order to retain as much data as possible using the original RINEX files, the current algorithm does not use the standard GIPSY data editor Turboedit. However, to identify cycle slips, the current algorithm uses the GIPSY module Sanity Edit (SanEdit). The cycle-slip criterion (set at 0.8 meter) is intentionally set loose in order to permit data processing when rapid ionospheric variations are present due to irregularities.

*The SanEdit Algorithm.* For each (possibly) continuous phase arc:

- (1) A polynomial fit is performed on the L1-L2 phase observables (L1-L2 is the ionospheric combination of GPS observables, also written as LI). The polynomial degree is  $4 + \lceil \text{length of arc in hours} \rceil$ .
- (2) The L1-L2 data (minus the fit) is examined for the largest jump between adjacent points.
- (3) If the largest jump is larger than the slip detection parameter, then that jump is interpreted either as an outlier or a cycle slip.

- (4) If a cycle slip or outlier is detected, repeat the entire process. If no slip or outlier is detected we may proceed.

Since the purpose of producing this truth data set is to study the storm-time ionospheric conditions, we need to keep as many data points as possible. In order for the editor to not remove data points, the slip detection parameter we are currently using in SanEdit is large (0.8 meters). Slips that small are rare — slips are typically very large. Therefore, we expect that SanEdit to be efficient in flagging cycle slips. We visually checked the processed data and found no obvious cycle slips remaining in the data.

We have chosen to use a slip parameter which is small, because then it would insert too many cycle slips: the accuracy of the “leveling” depends very much on the arc length and excessive slips degrades data accuracy, and very short arcs are typically of no use. However, of course, unflagged slips corrupt the data.

Furthermore, we remove data arcs less than 5 minutes in duration. We apply a 5-second smoothing window to smooth the 1-second pseudorange observations in order to mitigate multipath error on the code measurements.

*Leveling Phase Using Code Measurements.* The level is computed by averaging code minus phase ionospheric observables (PI-LI) using an elevation-dependent weighting. Higher elevation data is weighted more heavily. (The weighting is based on historical Turborogue PI-LI noise/multipath data giving a historical PI-LI scatter of  $\sigma_{th}(E)$  where  $E$  is elevation.) Specifically, the level is computed as

$$L = \frac{\sum_i \frac{1}{\sigma_{th}(E(t_i))^2} (PI(t_i) - LI(t_i))}{\sum_i \frac{1}{\sigma_{th}(E(t_i))^2}}, \quad (1)$$

where  $E$  is the elevation angle. The uncertainty on the level is computed using a combination of  $\sigma_{th}(E)$  and observed pseudorange scatter:

$$\text{Scatter from } \sigma_{th} = \sqrt{\frac{1}{N} \sum_i \sigma_{th}(E(t_i))^2}, \quad (2)$$

$$\text{True scatter} = \sqrt{\frac{1}{N-1} \sum_i (PI(t_i) - LI(t_i) - L)^2}, \quad (3)$$

where  $N$  is the number of data points. Note that for very short arcs, the elevation weighting has almost no effect on the average, and the level uncertainty approximately reverts to  $\text{Truescatter}/\sqrt{N}$ .

*Post-processing strategy.* After obtaining the 5 second leveled carrier phase ionospheric observables and the complete set of satellite and receiver interfrequency biases, we applied the biases to the ionospheric measurements to obtain un-biased phase-leveled ionospheric TEC measurements. We obtained TEC measurements separately for WAAS Reference Elements WRE1, WRE2 and WRE3 threads. In a subsequent step, we applied a voting scheme to select one of the three measurements as truth. We select one out of three data points or one out of two data points depending on the availability of three or two measurement threads. We also apply a 20% criterion, that all three threads agree within this range, when all three threads are available and a 40% criterion when only two threads are available (agreement of two threads within 40%). A TEC upper and lower bounds are also set as a sanity criteria. Finally, we set TEC sigma criterion to a loose 10 TECU criterion to minimize data loss.

### WAAS PLANAR FIT IONOSPHERIC MODEL

In the currently implemented WAAS ionospheric real-time correction algorithm, the vertical ionospheric delay is estimated at each ionospheric grid point by constructing a planar fit of a set of (bias-corrected) slant measurements projected to vertical:

$$TEC = M(h, E)[a_0 + a_1 d_E + a_2 d_N], \quad (4)$$

where

$a_0, a_1, a_2$  are the planar fit parameters;  
 $d_E, d_N$  are the distances from the IGP to the IPP in the eastern and northern directions, respectively.

Each least squares fit includes all IPPs that lie within a minimum fit radius surrounding the IGP. If the number of IPPs within this minimum radius is less than  $N_{min}$ , the fit radius  $R_{fit}$  is extended until it encompasses  $N_{min}$  points. In this study we do not tabulate data when the fit radius reaches its maximum value of  $R_{max}$  without having encompassed  $N_{min}$  points.  $R_{max}$  is chosen to be 2100 km which is the value in the current WAAS implementation.

In our WAAS estimation scheme (see Equation 4), we do not solve for the satellite and receiver differential biases. Instead, we use the GIM approach, to solve for high

precision differential biases, and we calibrate the ionospheric range measurements before applying Equation 4. This is similar to the approach used in WAAS.

### DATA ANALYSIS STRATEGY

In our data analysis, we treated every IPP data point as if it were collocated with a WAAS IGP (so-called “pseudo IGP” approach). Subsequently, we applied the WAAS planar fit ionospheric model algorithm to estimate the vertical ionospheric delays at each of these IPPs, treated as pseudo IGP values. Starting with the set of measurements that contributed to the planar fit, we then computed the residual difference between the slant measurements and the estimated slant delays based on the planar fit, projecting the vertical TEC from the planar estimate into the line-of-site using the WAAS thin-shell obliquity factor. This residuals analysis provides a measure of the performance of the planar fit algorithm in reproducing slant TEC for the user.

To investigate how ionospheric spatial gradients during the October storm event contribute to errors in the WAAS corrections in the CONUS, we looked at pairs of GPS receivers observing the same satellites at nearly identical elevation and azimuth angles. This approach was first reported in Komjathy et al., [2003b]. Here, we provide a short summary of the approach.

Vertical delay differences were computed after projecting the slant ionospheric range delay into the vertical. See Figure 1.

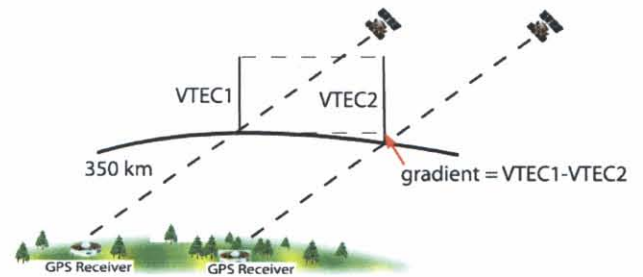


Figure 1. Illustration for computing ionospheric delay differences versus distance (gradient) for separated measurements with similar look angles.

We were also interested in finding out the potential range errors introduced by using the WAAS thin-shell mapping function during the October storm event. To do that we analyzed measurements for which the IPPs were nearly collocated but differed in elevation angle. Mapping function errors were computed by taking the difference between the

two slant ionospheric measurements, each projected to the vertical using the WAAS thin-shell mapping function.

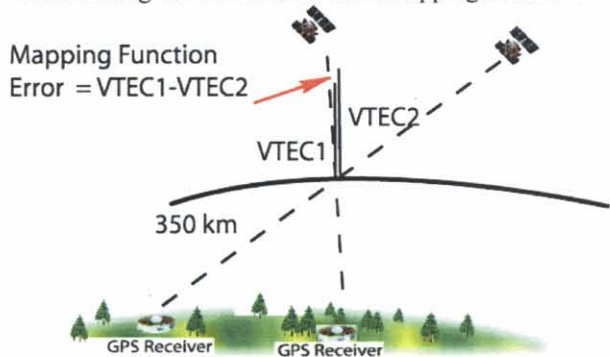


Figure 2. Illustration for computing mapping function error. Measurements with nearly collocated IPPs were differenced.

## DATA SETS

For our data set, we used the October 28-31, 2003 period when the geomagnetic storm occurred. October 28 was a quiet day and October 29-31, 2003 period was geomagnetically disturbed. In Figure 3, we show the locations of the WAAS Reference Sites (WRSs). At each location, we had three co-located receivers WAAS Reference Elements (WREs).



Figure 3. WRS locations each equipped with three WREs.

Interplanetary coronal mass ejections (ICMEs) were detected on October 29 and 30, 2003 that were related to X-class solar flares that occurred on October 28 and 29, 2003 as observed by ACE. The sheath reached the ACE satellite at 5:45 UT on October 29. The shock is identified by the sharp rise in velocity, temperature and magnetic field strength as seen in panels 1 to 4 in Figure 4. The postshock sheath showed highly fluctuating IMF  $B_z$

components resulting a first geomagnetic storm peak  $D_{st}$  of  $-159$  nT. The magnetic field orientation is highly irregular and so a mild geomagnetic storm response may be expected. In the bottom panel we observe that the Dst index begins to recover at 13:45 UT. However, another ( $2^{\text{nd}}$ ) geomagnetic storm begins during the recovery phase of the first storm causing a sudden Dst decrease on October 29. The  $B_z$  component (panel 5) continues to turn southward reaching a value of  $-30$  nT at 19:10 UT. This combined with solar wind velocities of 1200 km/sec causes a major geomagnetic storm (the  $2^{\text{nd}}$ ) and subsequently the Dst reaches  $-350$  nT at 01:25 UT on October 30. The shock of the second ICME occurs at 16:50 UT on October 30. The geomagnetic field  $B_z$  component causes a third geomagnetic storm that commences at 18:45 UT and reaches its maximum value of  $-390$  nT at 23:15 UT on October 30. The main topic of this paper is to investigate the impact of the storm events ( $2^{\text{nd}}$  and  $3^{\text{rd}}$ ) on the GPS data.

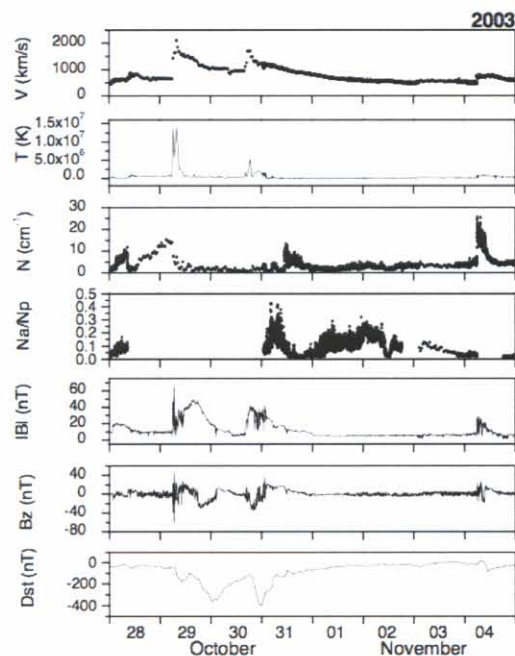


Figure 4. Changes in the geomagnetic field components during the October 28-31, 2003 period.

## ANALYSIS OF RESULTS

First we investigated the ionospheric slant delays and the WAAS planar fit residuals for the quiet day of October 28. In Figure 5 we plotted the slant ionospheric delays in blue and the planar fit slant residuals in red. The slant ionospheric delays are less than 35 meters and the WAAS planar fit residuals are less than 2 meters with an RMS of

0.4 TECU. Earlier, we had found 2 meter level planar fit residuals for quiet CONUS days (0.5 TECU RMS) using IGS and CORS data [Komjathy et al., 2002].

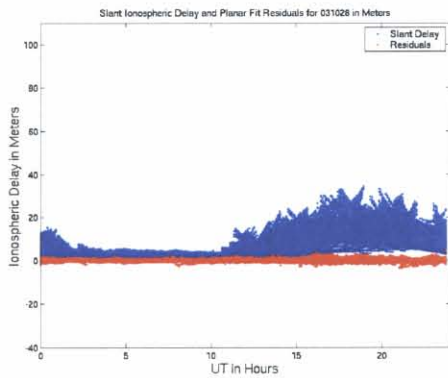


Figure 5. Slant Ionospheric delay and WAAS planar fit residuals for the quiet day of October 28, 2003.

When comparing the time series between October 28 and 29, we observe similar ionospheric delays and planar fit residuals prior to 19:00 UT when after the geomagnetic field  $B_z$  component reaches  $-30$  nT at around 19:10 UT. With the combination of high solar wind velocities and the  $B_z$  component turning southward, the geomagnetic storm reached its maximum strength with a  $D_{st}$  index of  $-350$  nT at 01:25 UT on October 30. In Figure 5, this can be characterized with slant ionospheric delays at the 100 meter level, an increase of factor of 3 compared to quiet time conditions. The planar fit residuals increased by an order of magnitude. The slant planar fit residuals are less than 20 meters with an RMS of 2.6 meters for October 29 as opposed to about 2 meters (0.4 meter RMS) for the quiet previous day.

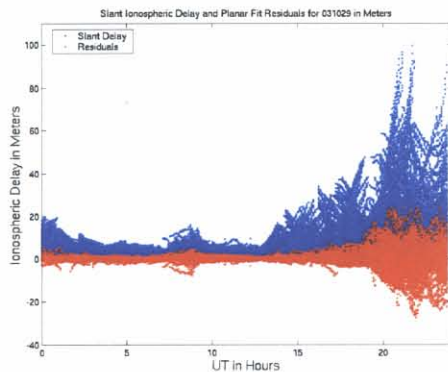


Figure 6. Ionospheric delays and WAAS planar fit residuals for October 29, the first storm day.

At the early hours of October 30, we observe unusually high ionospheric activity corresponding to pre-midnight conditions in the CONUS. After about 02:00 UT, the storm

activity subsides corresponding to the recovery phase of the first storm.

With the onset of the second ICME occurring around 16:50 UT on October 30, we see the increased ionospheric delays. As the geomagnetic field  $B_z$  component continues to turn southward, the third geomagnetic storm commences at 18:45 UT reaching its full strength at 23:15 UT. This is observed in Figure 7, where the ionospheric delays reach values larger than 100 meters with planar fit residuals exceeding 25 meters. The RMS of the planar fit residuals for October 30 turned out to be as large as 3.4 meters.

In the early hours of October 31, the third storm starts its recovery phase slowly decreasing ionospheric delays and planar fit residuals returning to quiet conditions around 10 UT (Figure 8).

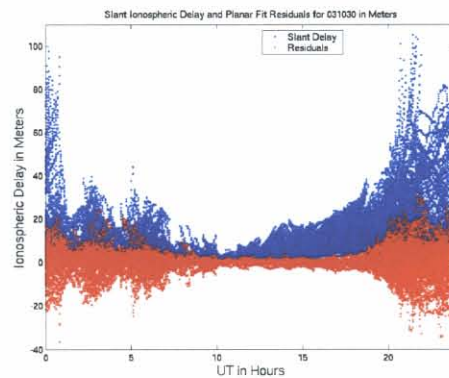


Figure 7. Ionospheric delays and planar fit residuals for October 30.

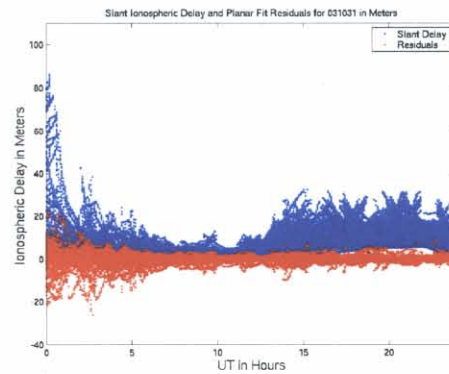


Figure 8. Ionospheric delays and planar fit residuals for October 31.

*Characterizing WAAS ionospheric delay differences.* We generated data points by selecting pairs of stations observing the same satellites at nearly identical elevation and azimuth angles. We computed vertical delay gradients

by differencing the vertical TEC from these stations and tabulating the distance between them. The slant delays are converted to vertical using the WAAS obliquity scaling factor (thin shell at 350 km).

*Delay difference between two receivers: time series for a quiet day.* We show an example in Figure 9, displaying the difference between measured ionospheric delay for two receivers observing the same satellite at similar azimuth and elevation angle. We limited the maximum separation between IPPs to 1000 km. We found that the delay differences in CONUS can reach 3 meters over 700 km for the quiet day. In Figure 10, we can clearly see the diurnal variation of the delay differences for the quiet October 8 day.

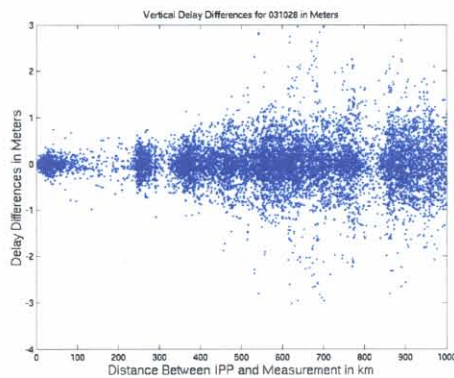


Figure 9. Measured vertical delay differences for nearby receivers for the quiet day of October 28, 2003.

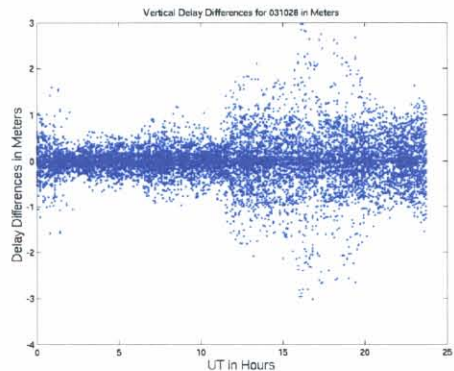


Figure 10. Diurnal variation of the measured vertical delay differences for nearby receivers for the quiet day of October 28, 2003.

In Figure 11, we have chosen the storm day of October 30 to demonstrate the delays differences during intense storm conditions. The delay differences can be as high as 25 meters over 700 km. This is an order of magnitude increase compared to the quiet time conditions depicted in

Figure 9. As a reference, we also plotted the quiet day time series of October 28. This is shown in red in Figure 11.

In Figure 12, we display the diurnal variation of the delay differences showing the slight differences between the delay differences as a result of the second (early hours of Figure 11) and third geomagnetic storm (late hours in Figure 11). We again overlapped the time series with the values of the quiet day conditions indicating an order of magnitude increase during storm time.

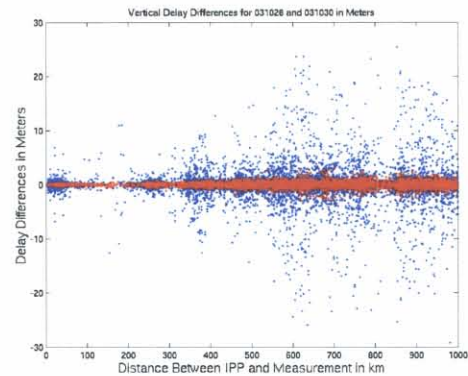


Figure 11. Measured vertical delay differences for nearby receivers for the quiet day of October 30, 2003.

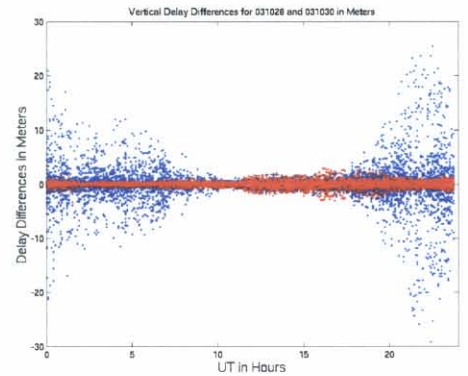


Figure 12. Diurnal variation of the measured vertical delay differences for nearby receivers for the quiet day of October 30, 2003.

*Mapping function error.* As another potential error source, we explored the errors introduced by the thin-shell ionospheric mapping function. The idea is to find pairs of observations from different receivers with nearly collocated IPPs. If the elevation mapping function contains no errors, the two slant observations should provide us with identical vertical range delays. In fact, mapping function errors are present and assessed by projecting the two slant observations into the vertical using the respective elevation angles and subsequently taking the difference between the two nearly collocated vertical estimates (for illustration see Figure 2).

In Figure 13, we plotted the mapping function errors as a function of elevation angle. The data points in blue represent the October 30 conditions showing little elevation angle dependence during storm conditions. In red the quiet time conditions show elevation angle dependence as expected. The mapping function error appears to be as large as 10 meters for the October 30 storm day. In Figure 14, we plot the diurnal variation of the mapping function error. It shows that the third geomagnetic storm (last hours in the plot) showed the largest 10 meter level mapping function error. The largest error during storm time is a factor of 12 times larger than the maximum error during quiet time.

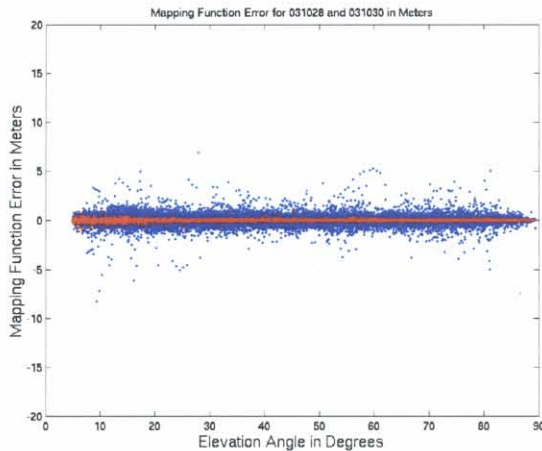


Figure 13. Mapping Function error for quiet and storm time as a function of elevation angle.

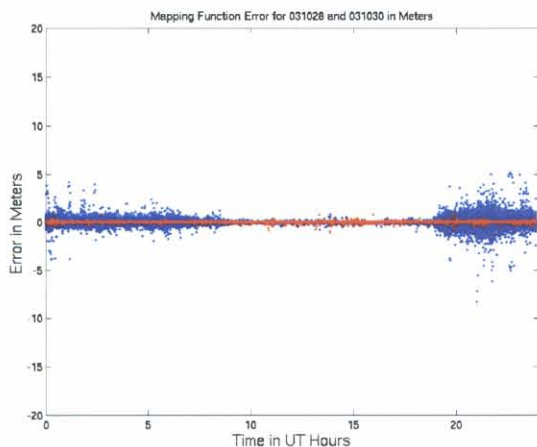


Figure 14. Diurnal variation of mapping function error for quiet and storm time.

*Implications for LNAV/VNAV availability.* We have investigated ionospheric range errors in the mid-latitude CONUS for quiet and storm days of the period between

October 28 and 31, 2003. Based on this limited data set, we found that using a tuned variant of the WAAS planar fit algorithm, the residuals are less than 2 meters (0.4 meter RMS) for the quiet day and less than 20 meters (3.4 meter RMS) for intense storm day. This has major implications for availability of the initial WAAS Lateral Navigation/Vertical Navigation service (LNAV/VNAV). The user determines, in real-time, the level of navigation service available based on the broadcast grid ionosphere vertical errors (GIVEs) and other information. GIVE values represent 3.29-sigma bounds on vertical ionosphere range error at each ionospheric grid point. Service volume model studies for WAAS have shown that high availability of LNAV/VNAV service is possible when a significant majority of the broadcast GIVEs are in the range 3-6 meters.

During storm conditions, the GIVEs must be increased to cover the larger ionospheric range errors expected. Increased planar fit residuals from quiet time to storm time by a factor of eight are likely to result in large number of GIVEs above 6 meters. Due to the GIVE quantization, computed GIVEs above 6 meters are transmitted as 15-meter bounds to the user. As a result, LNAV/VNAV service will be unavailable if several of the users' satellite links are associated with GIVEs of 15 meters or more.

## CONCLUSIONS

In this paper, we investigated the performance of the WAAS planar fit correction algorithm in the CONUS during quiet and storm conditions using data sets between one of the largest geomagnetic storm period in recent history.

We found ionospheric range delays up to 35 meters for the day-time CONUS during quiet and up to 100 meters during storm time conditions. For quiet day, we obtained WAAS planar fit residuals less than 2 meters (0.4 meter RMS) and less than 20 meters (3.5 meter RMS) for the storm day.

For CONUS we found ionospheric gradients, averaged over a distances of a few hundred km, were no larger than 0.5 meter over 100 km for a quiet day. For storm days, we found gradients at the 4 meter level over 100 km. Similar level gradients could otherwise only be observed in low latitude region.

Errors associated with mapping slant observations to vertical resulted in errors less than 0.8 meters (4 cm RMS) for quiet days and less than 10 meters (35 cm RMS) for the storm days corresponding to an order of magnitude change.

It appears that the inherent spatial and temporal variability of the ionosphere is driving the residual errors during storm conditions in the CONUS region using the current WAAS algorithm. This size or magnitude of the residuals, gradients and mapping errors are similar or larger than those observed during quiet or storm conditions in the low latitude region. Since this data set is representative for low solar activity conditions the error are expected to increase during storm conditions in high solar activity conditions.

Our previous studies in middle and low latitude regions relied on dual-frequency GPS data from CORS, IGS and Brazilian sites with no redundant observations available. With no redundancy, robust data editing algorithms were applied to remove outliers, but it is possible that some valid data was rejected, or marginally poor data was accepted. With the current truth data set, we are confident that no data was rejected and so the remaining data points may be considered representative for quiet and storm time conditions in the CONUS region. Considering the fact that the triple redundant truth data set resulted in similar RMS of residuals for middle latitude during quiet and storm times to results reported earlier [Komjathy et al., 2003b, 2003c], it is likely that previous data set using CORS and IGS did not miss important ionospheric features during storm times. The three co-located GPS receivers we applied in this research have helped prove the validity of our extensive previous reported data processing efforts using data from CORS and IGS networks.

## ACKNOWLEDGMENT

This research was performed at the Jet Propulsion Laboratory/California Institute of Technology under contract to the National Aeronautics and Space Administration and the Federal Aviation Administration.

## REFERENCES

Blanch, J., T. Walter and P. Enge. (2002). "Application of Spatial Statistics to Ionosphere Estimation for WAAS." *On the CD-ROM of the Proceedings of the National Technical Meeting of the Institute of Navigation*, San Diego, CA, January 28-30.

Enge, P., T. Walter, S. Pullen, C. Kee, Y.C. Chao and Y.-J. Tsai (1996). "Wide Area Augmentation of the Global Positioning System." *Proceedings of the IEEE*, Vol. 84, pp. 1063-1088.

Iijima, B.A., I.L. Harris, C.M. Ho, U.J. Lindqwister, A.J. Mannucci, X. Pi, M.J. Reyes, L.C. Sparks, B.D. Wilson

(1999). "Automated Daily Process for Global Ionospheric Total Electron Content Maps and Satellite Ocean Altimeter Ionospheric Calibration Based on Global Positioning System." *Journal of Atmospheric and Solar-Terrestrial Physics*, Vol. 61, pp. 1205-1218.

Komjathy, A., B.D. Wilson, T.F. Runge, B.M. Boulat, A.J. Mannucci, L. Sparks and M.J. Reyes (2002). "A New Ionospheric Model for Wide Area Differential GPS: The Multiple Shell Approach." *On the CD-ROM of the Proceedings of the National Technical Meeting of the Institute of Navigation*, San Diego, CA, January 28-30.

Komjathy, A. Sparks, L., Mannucci, A.J., and X. Pi (2003a). "An Alternative Ionospheric Correction Algorithm for Satellite-Based Augmentation Systems in Low-latitude Region." *On the CD-ROM of the Proceedings of GNSS 2003 The European Navigation Conference*, April 22-25, Graz, Austria.

Komjathy, A., L. Sparks, A.J. Mannucci and X. Pi (2003b). "An Assessment of the Current WAAS Ionospheric Correction Algorithm in the South American Region" *NAVIGATION: Journal of the Institute of Navigation*, Vol 50, No. 3, Fall 2003, pp. 193-204.

Komjathy, A., L. Sparks, T. Mannucci (2003c). "On the Ionospheric Impact of Recent Storm Events on Satellite-Based Augmentation Systems in the Middle and Low-latitude Regions, On the CD-ROM of the 2003 International Technical Meeting of the Institute of Navigation, Sept 9-12, 2003, Portland, OR,

Lawson, C. (1984). "A Piecewise C2 Basis for Function Representation over a Surface of a Sphere." JPL internal document.

Mannucci, A.J., B.D. Wilson, D.N. Yuan, C.H. Ho, U.J. Lindqwister and T.F. Runge (1998). "A Global Mapping Technique for GPS-derived Ionospheric Total Electron Content Measurements." *Radio Science*, Vol.33, pp.565-582.

Mannucci A.J., B.A. Iijima, L. Sparks, X. Pi, B.D. Wilson and U.J. Lindqwister (1999). "Assessment of Global TEC Mapping Using a Three-Dimensional Electron Density Model." *Journal of Atmospheric and Solar Terrestrial Physics*, Vol. 61, pp. 1227-1236.

Sparks, L., B.A. Iijima, A.J. Mannucci, X. Pi, B.D. Wilson (2000). "A New Model for Retrieving Slant TEC Corrections for Wide Area Differential GPS." *Proceedings*

*of the ION National Technical Meeting 2000 of the Institute of Navigation, Anaheim, CA, 26-28 January, pp. 464-474.*

Sparks L., A. Komjathy, A. J. Mannucci (2004a). "Sudden Ionospheric Delay Decorrelation and its Impact on the Wide Area Augmentation System (WAAS)," *Radio Science*, 39, RS1S13,

Sparks, L., A. Komjathy, A.J. Mannucci (2004b). "Estimating SBAS Ionospheric Delays without Grids: The Conical Domain Approach." On the CD-ROM of the ION 2004 National Technical Meeting, San Diego, CA, January 26-28, 2004.

WAAS MOPS (1999). "Minimum Operational Performance Standards for Global Positioning System/Wide Area Augmentation System Airborne Equipment." RTCA Inc. Document No. RTCA/DO-229B October 6. pp 225.

Walter, T., A. Hansen, J. Blanch, P. Enge, T.J. Mannucci, X. Pi, L. Sparks, B. Iijima, B. El-Arini, R. Lejeune, M. Hagen, E. Altschuler, R. Fries, A. Chu (2000). "Robust Detection of Ionospheric Irregularities." *On the CD-ROM of the Proceedings of ION GPS 2000, 13th International Technical Meeting of the Institute of Navigation, Salt Lake City, UT, 11-14 September.*